Long non-coding RNAs lnc-ANGPTL1-3:3 and lnc-GJA10-12:1 present as regulators of sentinel lymph node metastasis in breast cancer

DESHENG SUN[1], JIEYU ZHONG[1], WEI WEI[2], LI LIU[1], JUN LIU[3] and XIAONA LIN[1]

Departments of [1]Ultrasonography, [2]Breast Surgery and [3]Pathology, Peking University Shenzhen Hospital, Shenzhen, Guangdong 518036, P.R. China

Received September 27, 2019; Accepted June 12, 2020

DOI: 10.3892/ol.2020.12050

Abstract. Long non-coding RNAs (lncRNAs) participate in various biological processed involved in tumorigenesis, metastasis and proliferation. The aim of the present study was to identify candidate long non-coding RNAs (lncRNAs) involved in sentinel lymph node (SLN) metastasis in breast cancer. Specimens of SLNs were collected from patients with SLN metastasis via punch biopsy. Total RNA was extracted and RNA sequencing (RNA-seq) was conducted. Differential expression profiles of mRNAs and lncRNAs were obtained via bioinformatics analysis, and Gene Oncology (GO) and Kyoto Encyclopedia of Genes and Genomes (KEGG) analyses were performed on differentially expressed mRNAs. The expression levels of lncRNAs were analyzed via reverse transcription-quantitative PCR (RT-qPCR), and the regulation network of the lncRNAs to downstream microRNAs (miRs) and mRNAs was predicted. Based on RNA-seq results, six differentially expressed candidate lncRNAs were identified in patients with and without SLN metastasis: lnc-ANGPTL1-3:3, lnc-GJA10-12:1, lnc-ACAN-2:1, lnc-ZPBP2-4:1, lnc-GATA3-16:1 and lnc-ACOX3-5:1. KEGG and GO analysis identified that the mitogen-activated protein kinase (MAPK) and PI3K/Akt signaling pathways were the most enriched pathways. After RT-qPCR analysis, lnc-ANGPTL1-3:3 and lnc-GJA10-12:1 exhibited expression patterns that were consistent with those from RNA-seq. Moreover, receiver operating characteristic curve analysis demonstrated that lnc-ANGPTL1-3:3 and lnc-GJA10-12:1 expression levels had high sensitivity and specificity in the diagnosis of SLN metastasis, and that their expression levels were upregulated in patients with axillary lymph node metastasis. Further analysis revealed that lnc-GJA10-12:1 and lnc-ANGPTL1-3:3 were commonly involved in regulating the miR-302 family, including miR-302d-3p and miR-302c-3p, which together targeted AKT1. Additionally, lnc-ANGPTL1-3:3 was predicted to target miR-520b to regulate MAP3K2 expression. lnc-GJA10-12:1 was also predicted to target miR-34a-5p to regulate MAP2K1 and MAP3K9 expression levels, as well as miR-449a to regulate MAP2K1 expression. The results of the present study suggested that lnc-ANGPTL1-3:3 and lnc-GJA10-12:1 may potentially serve a role in SLN metastasis of breast cancer by regulating the PI3K/Akt and MAPK signaling pathways via targeting the miR-302 family, miR-520a-3p, miR-34a-5p and miR-449a. Thus, lnc-ANGPTL1-3:3 and lnc-GJA10-12:1 in SLN may serve as potential markers of breast cancer metastasis.

Introduction

In the Global Cancer Statistical Analysis of 2018, the number of breast cancer cases was 2,088,849, which was only lower than the number of lung cancer cases, however, due to the relatively good prognosis the number of deaths from breast cancer was much lower compared with those from lung cancer (1). The disease status of the axillary lymph nodes is the most important prognostic factor for patients with early-stage breast cancer (2). The most common predictors of node metastasis include lymphovascular invasion, age, tumor size and tumor grade; additionally, the predictive value is influenced by casting-type calcifications on mammography, receptor states, tumor location and the method of detection (3-8). However, no combination of these predictors of axillary lymph node status can currently replace histopathology and the surgical resection of lymph nodes (9). Moreover, the histopathological diagnosis of removed lymph nodes via axillary lymph node dissection is thought to be the most effective method to assess the disease (10). Unfortunately, the anatomical disruption caused by axillary lymph node dissection can result in side effects, such as nerve injury, lymphedema and other complications (11).

It has been demonstrated that breast cancer usually spreads to one or a few lymph nodes, known as the sentinel lymph nodes (SLNs), before spreading to other axillary nodes (12).

Correspondence to: Ms. Jieyu Zhong, Department of Ultrasonography, Peking University Shenzhen Hospital, 1,120 North Lianhua Road, Futian, Shenzhen, Guangdong 518036, P.R. China
E-mail: zhongjieyu0717@163.com

Key words: breast cancer, sentinel lymph node, metastasis, mitogen-activated protein kinase

Therefore, the use of SLN identification and sampling procedures, referred to as SLN biopsies, can be a reliable treatment strategy in patients with early-stage breast cancer, as it reduces the need for axillary lymph node dissection and avoids the associated morbidity (13-17). Based on the aforementioned principles, SLN metastasis detection may be a key method for assessing the spread of breast cancer to the axillary lymph nodes. However, the underlying molecular mechanism of SLN metastasis in breast cancer remains unknown.

Long non-coding RNAs (lncRNAs) are non-protein coding transcripts of >200 nucleotides in length. Previous studies have reported that lncRNAs participate in various biological processes involved in tumorigenesis, metastasis and proliferation (18-21). Therefore, lncRNAs may be considered as diagnostic biomarkers for numerous types of cancer, such as gastric, bladder, colorectum and prostate cancer (22-25). For example, lncRNA-BANCR has been associated with lymph node metastasis in colorectal cancer (26). The function of lncRNAs in breast cancer has also been studied. For instance, lncRNA-SNHG15 regulates microRNA (miRNA/miR)-211-3p and promotes cell proliferation, migration and invasion of breast cancer (27). Additionally, lncRNA-MAPT-AS1 inhibits cell proliferation and migration by regulating MAPT expression in breast cancer (28). Therefore, the aforementioned studies have indicated that lncRNAs may be important for regulating breast cancer processes and may be potential biomarkers of the disease. However, the role served by lncRNAs in SLN metastasis of breast cancer is yet to be elucidated.

To screen for markers that can be used to identify whether SLN has metastasized in breast cancer, in the present study, the SLNs of patients with breast cancer were collected and RNA sequencing (RNA-seq) was used to identify the key lncRNAs involved in SLN metastasis. Furthermore, reverse transcription-quantitative PCR (RT-qPCR) was conducted to analyze the expression levels of lncRNAs among specimens with or without SLN metastasis.

Materials and methods

Patient review and specimen collection. The database of the Peking University Shenzhen Hospital (Shenzhen, China) was reviewed between January 2018 and December 2018 in breast cancer, and patients in the early stages (I and II) of breast cancer were included in the present study. The patients were >18 years old, had not received surgical contraindication, chemotherapy or endocrine therapy, and had no other malignancy or immune diseases. Samples were obtained from 46 patients with an age range of 26-72 years. The mean age of 26 patients with SLN metastasis was 47±2.726 years and that of 20 patients without SLN metastasis was 47±3.674 years. All the patients were female. Patients were studied prospectively and data were collected with regards to age; metastasis-relevant parameters including disease history, tumor position, lymph node metastasis by sentinel lymph node biopsy (SLNB) and pattern of the axillary lymph nodes; and TNM stage according to the guidelines from the American Joint Committee on Cancer (29). Mammary areola injection was performed for the ultrasound contrast to search for SLNs. Subsequently, punch biopsy was conducted in order to collect the specimens. The patients underwent breast cancer resection and intraoperative SLN biopsy within 48 h of puncture. The present study was approved by the Institute Research Medical Ethics Committee of the Peking University Shenzhen Hospital, and informed consent was provided orally and in writing by all patients.

RNA-seq. Total RNA from the tissues was purified using an RNeasy Mini kit (Qiagen GmbH). RNA integrity was evaluated based on the RNA integrity number (RIN) value using an Agilent Bioanalyzer 2100 (Agilent Technologies, Inc.). RNA clean-up was performed using an RNA Clean XP kit (Beckman Coulter, Inc.) and the DNA residue was removed with an RNase-free DNase Set (Qiagen GmbH). The quality and concentration of the RNA were determined using NanoDrop 2000 (Thermo Fisher Scientific, Inc.). The ribosomal RNA was removed using a NEBNext rRNA Depletion kit (New England BioLabs, Inc.). Subsequently, 1 μg total RNA was used for library preparation using a VAHTSTM mRNA-seq v2 library Prep kit (Vazyme Biotech Co., Ltd.), according to the manufacturer's protocol. Briefly, the RNA was fragmented and the double strand cDNA was synthesized. Subsequently, end-polishing was performed and the cDNA fragments were ligated with adapters. The ligated cDNA was amplified using 15 cycles of PCR for 10 sec at 98˚C, 30 sec at 60˚C and 30 s at 72˚C using a PCR master mixture (Illumina, Inc.) and subjected to universal PCR amplification using DNA polymerase I (New England BioLabs, Inc.) in order to obtain a library sufficient for sequencing. The Agilent Bioanalyzer 2100 was used to evaluate the quality of the library and an Illumina Hiseq 4000 (Illumina, Inc.) was used for RNA-seq. SOAP (http://soap.genomics.org.cn/) was used to calculate lncRNAs and mRNAs expression. Differentially expressed lncRNAs and mRNAs were screened using R software version 3.1 (30) according to the following criteria: False discovery rate (FDR) ≤0.001 and fold-change >2.

Gene Ontology (GO) and Kyoto Encyclopedia of Genes and Genomes (KEGG) pathway analysis. The Database for Annotation, Visualization and Integrated Discovery (https://david.ncifcrf.gov/) was used to annotate the potential functions in various signaling pathways of the differentially expressed mRNAs. Subsequently, the functional annotation of parental genes was predicted via GO functional annotation (http://geneontology.org/page/go-enrichment-analyses). KEGG pathway annotation (http://www.genome.jp/kegg/pathway.html) was also used to identify the relevant pathways of the differentially expressed mRNAs.

RT-qPCR. Six lncRNAs with lengths of 500-3,000 bp were selected for assessment based on information from the lncRNASNP2 database (http://bioinfo.life.hust.edu.cn/lncRNASNP/) and their predicted association with breast cancer. lncRNA expression levels were verified by RT-qPCR. RNA was extracted according to the above RNA-seq method. Gene expression was analyzed via RT-qPCR. RNA was reverse-transcribed into cDNA using the cDNA Synthesis Kit system (Promega Corporation) according to the manufacturer's protocol at 42˚C for 15 min and then 95˚C for 3 min. The qPCR reaction was performed using GoTaq qPCR Master mix (Promega Corporation), and qPCR amplification was performed using an ABI 7500 system (Applied Biosystems;

Table I. Primers used for quantitative PCR.

Gene	Sequence, 5'→ 3'	Product length, bp
lnc-ACAN-2:1	F: CAAAGGGGAGCCAAGGTAGG	149
	R: GGGTGAGCGTTCAGATTCCA	
lnc-ZPBP2-4:1	F: CCTAGACGGCAGCTTAGGAC	100
	R: TTGTGGCAGTGTAAACCCCT	
lnc-GATA3-16:1	F: CGAGGAGGCAGTGTGACAAA	178
	R: CTCTAGGAAGTGGAGGCACC	
lnc-ACOX3-5:1	F: TTCATCATCTCGTGGGACGC	96
	R: GTGTCCAGCCTATTGGGACC	
lnc-ANGPTL1-3:3	F: AGTTGGGGACGCTAGAATGC	109
	R: TGTTGCCTATCCTCGCTGTT	
lnc-GJA10-12:1	F: TCCAAGCTGTCCTGTACGAAG	99
	R: GCTGCTGATGCAAGCTGAAA	
GAPDH	F: GTCTCCTCTGACTTCAACAGCG	235
	R: ACCACCCTGTTGCTGTAGCCAA	

F, forward; R, reverse; lnc, long non-coding RNA.

Thermo Fisher Scientific, Inc.). Thermocycling conditions for qPCR were as follows: 40 cycles of 20 sec at 95˚C followed by 30 sed at 60˚C and 30 sec at 72˚C. The relative mRNA expression levels were calculated by $2^{-\Delta\Delta Cq}$ method (31). Primers for qPCR are presented in Table I. GAPDH was used as an internal control.

Statistical analysis. The data from three experimental repeats was shown as mean ± standard deviation. Data comparisons were performed using unpaired Student's t-tests and χ^2 tests. Receiver operating characteristic (ROC) curve was drawn to analyze the specificity and sensitivity of lncRNA as a disease diagnosis. $P<0.05$ was considered to indicate a statistically significant difference. SPSS version 19.0 (IBM Corp.) and GraphPad Prism 8 (GraphPad Software, Inc.) were used to conduct the statistical analyses.

Results

Characteristics of the patients involved in the present study. The inclusion criteria for the present study were patients diagnosed with breast cancer and those suitable for axillary lymph node dissection. The reagent for contrast-enhanced ultrasound was subcutaneously injected near the mammary areola to search for the position of the SLN biopsy. The patients were categorized into SLN(+) or SLN(-) metastasis groups and their characteristics are summarized in Table II. Analysis of the data identified that the positive rate of SLN metastasis was associated with the pattern of the axillary lymph nodes ($P=0.0001$), but was not associated with age, disease history, tumor position, molecular subtyping of breast cancer or TNM stage (all $P>0.05$; Table II).

Analysis of differentially expressed lncRNAs and mRNAs associated with SLN(+) and SLN(-) metastasis. The differentially expressed lncRNAs and mRNAs in patients with SLN(+) metastasis and SLN(-) metastasis are presented in Figs. 1 and 2 as volcano plots, scatter plots and heatmaps. A total of 2,335 differentially expressed lncRNAs were identified between patients with SLN(+/-) metastasis; of these, 1,120 were upregulated and 1,215 were downregulated (Fig. 1A-C; Table SI). Furthermore, the expression levels of lncRNAs on different chromosomes were both upregulated and downregulated (Fig. 1D). A total of 2,335 differentially expressed mRNAs were found between patients with SLN(+/-) metastasis; of these, 1,120 were upregulated and 1,215 were downregulated (Fig. 2A-C and Table SII). The Reads Per Kilobase of transcript per Million mapped reads profiles for lncRNAs and mRNAs were summarized and a fold-change >2 was used as a selection criterion to screen significantly differentially expressed lncRNAs and mRNAs. The top ten upregulated and downregulated lncRNAs and mRNAs are summarized in Tables III and IV, respectively.

Functional analysis of differentially expressed genes. GO annotation analysis was used to examine the processes in which the differentially expressed mRNAs were involved. The majority of these mRNAs were involved in 'cell differentiation', 'cell proliferation', 'immune response', 'cell death', 'cell migration' and 'mitogen-activated protein kinase (MAPK) cascade', but a few were also involved in the 'Wnt signaling pathway' and the 'apoptotic signaling pathway' (Fig. 2D). In order to assess the pathways in which the mRNAs were involved, KEGG pathway annotation analysis was conducted; the results revealed that the 'PI3K/Akt signaling pathway', 'Rhoptry-associated protein1 (Rap1) signaling pathway' and 'MAPK signaling pathway' were the main enriched pathways (Fig. 2E), suggesting that these were the primary signaling pathways in which mRNAs were involved.

Validation of lncRNA expression levels in patients with SLN(+) and SLN(-) metastasis. In the present

Table II. Clinicopathological parameters of patients with (n=26) and without (n=20) SLN metastasis.

Parameter	SLN(+)	SLN(+) NA	SLN(-)	SLN(-) NA	P-value
Cases	26	-	20	-	
Mean age ± SD, years	47.27±2.726	-	47.60±3.674	-	0.9414
Disease history, year					
≤1	19	-	15	-	0.8211
>1	7	-	5	-	
Tumor position					
Left breast	17	-	13	-	0.9783
Right breast	9	-	7	-	
Lymph node metastasis by SLN biopsy					
+	26	-	1	-	<0.0001
-	0	-	19	-	
Pattern of the axillary lymph nodes					
Non-suspicious	1	-	12	-	
Suspicious	25	-	8	-	
Human epidermal growth factor receptor 2					
+	3	9	1	1	0.5162
-	14		18		
Triple negative breast cancer					
+	0	9	3	1	0.2310
-	17		16		
Luminal A					
+	0	9	2	1	0.4873
-	17		17		
Luminal B					
+	14	9	13	1	0.5631
-	3		6		
Tumor size, cm					
<2	1	-	5	-	0.0949
≥2	25	-	15	-	
N stage					
N0	7	-	11	-	0.0531
N1	19	-	9	-	
M stage					
M0	25	-	20	-	1.0000
M1	1	-	0	-	

T, tumor; N, node; M, metastasis; SLN, sentinel lymph node; NA, Not available.

study, the differentially expressed lncRNAs, including lnc-ANGPTL1-3:3, lnc-GJA10-12:1, lnc-ACAN-2:1, lnc-ZPBP2-4:1, lnc-GATA3-16:1 and lnc-ACOX3-5:1 were analyzed by qPCR. As shown in Fig. 3, the expression levels of lnc-ANGPTL1-3:3, lnc-GJA10-12:1, lnc-ACAN-2:1 and lnc-ZPBP2-4:1 were significantly downregulated in the SLN (+) group compared with the SLN (-) groups. However, only the expression results of lnc-ANGPTL1-3:3 and lnc-GJA10-12:1 were confirmed using RNA-seq, while the results for lnc-ACAN-2:1 and lnc-ZPBP2-4:1 expression were the opposite to those obtained via RNA-seq (Table SI). It was also found that lnc-GATA3-16:1 and lnc-ACOX3-5:1 did not exhibit significant differential expression levels according to the qPCR results (Fig. 3).

Receiver operating characteristic (ROC) curve analysis identified that both lnc-ANGPTL1-3:3 and lnc-GJA10-12:1 had high area under the curve values (>0.8), which indicated that both lncRNAs were closely associated with SLN metastasis and may be suitable biomarkers for SLN diagnosis (Fig. 4). According to associations of lnc-ANGPTL1-3:3 and lnc-GJA10-12-1 expression levels with pathological features, lnc-ANGPTL1-3:3 and lnc-GJA10-12:1 expression levels were highly associated with patients with axillary lymph node metastasis or SLN metastasis diagnosis (Table V).

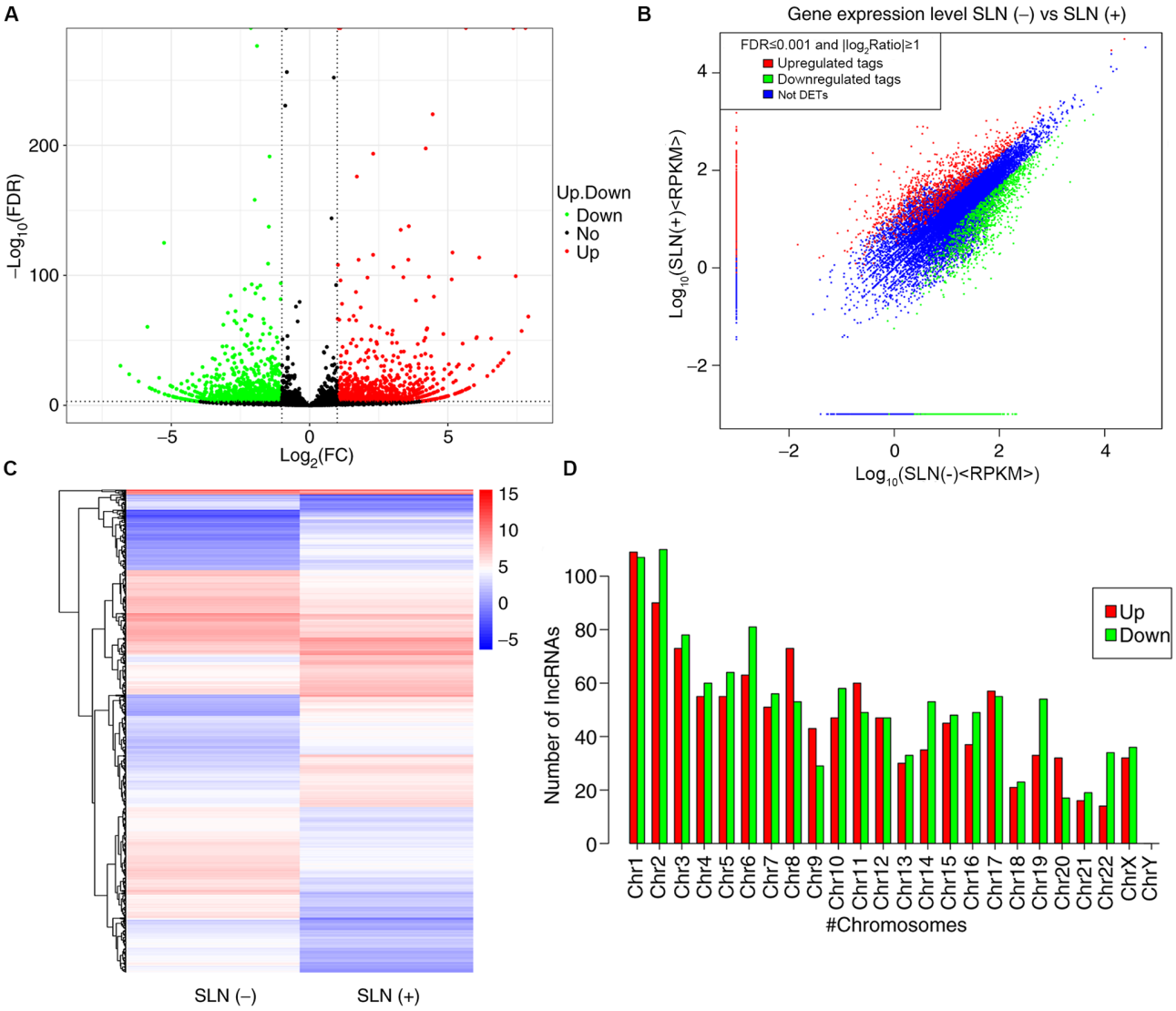

Figure 1. Differentially expressed lncRNAs in patients with SLN(+) and SLN(-) metastasis. (A) Volcano plot, (B) scatter plot and (C) heatmap (the color indicates the value after the logarithm of the expression is taken; the red color indicates higher gene expression and the bluer color indicates lower gene expression) of the differentially expressed lncRNAs in patients with SLN(+) and SLN(-) metastasis. (D) Distribution map of lncRNAs in different chromosomes. lncRNA, long non-coding RNA; SLN, sentinel lymph node; FDR, false discovery rate; FC, fold change; RPKM, Reads Per Kilobase of transcript per Million mapped reads; DETs, Differentially expressed tags; chr, chromosome.

Co-expression network analysis of lncRNAs and mRNAs. After ROC analysis and verification using qPCR, lnc-ANGPTL1-3:3 and lnc-GJA10-12:1 were selected for functional prediction analysis, in which the targets of these lncRNAs were predicted based on the competing endogenous RNA (ceRNA) principle (32). The target genes of lncRNAs, which were significantly downregulated in the SLN (+) group in mRNA sequencing compared with the SLN (-) group, in the top five pathways in the KEGG pathway analysis based on the ceRNA principle were used to establish network regulatory maps. The miRNAs that interacted with lncRNAs were predicted based on the sequences of lncRNAs, and the targets of miRNAs were thus also predicted. Under this principle, lncRNA-miRNA-mRNA cascades were identified. The top ten miRNAs and their corresponding targeted mRNAs associated with either lnc-ANGPTL1-3:3 or lnc-GJA10-12:1 are presented in Tables VI and VII, respectively. Moreover, the interactions are summarized in the regulation network illustrated in Fig. 5. The results demonstrated that the miRNAs associated with lnc-GJA10-12:1 and lnc-ANGPTL1-3:3 were commonly involved in regulating the miR-302 family, including miR-302d-3p and miR-302c-3p, which together targeted AKT1. Specifically, lnc-ANGPTL1-3:3 was predicted to target miR-520b to regulate MAP3K2 expression. In addition, lnc-GJA10-12:1 was predicted to target miR-34a-5p to regulate MAP2K1 and MAP3K9 expression, as well as miR-449a to regulate MAP2K1 expression. Therefore, the results indicated that lnc-GJA10-12:1 and lnc-ANGPTL1-3:3 may be involved in signal conditioning networks to control SLN metastasis in breast cancer.

Discussion

In the present study, RNA-seq was performed to identify the lncRNAs involved in the SLN metastasis processes in breast cancer. According to the qPCR results, lnc-ANGPTL1-3:3

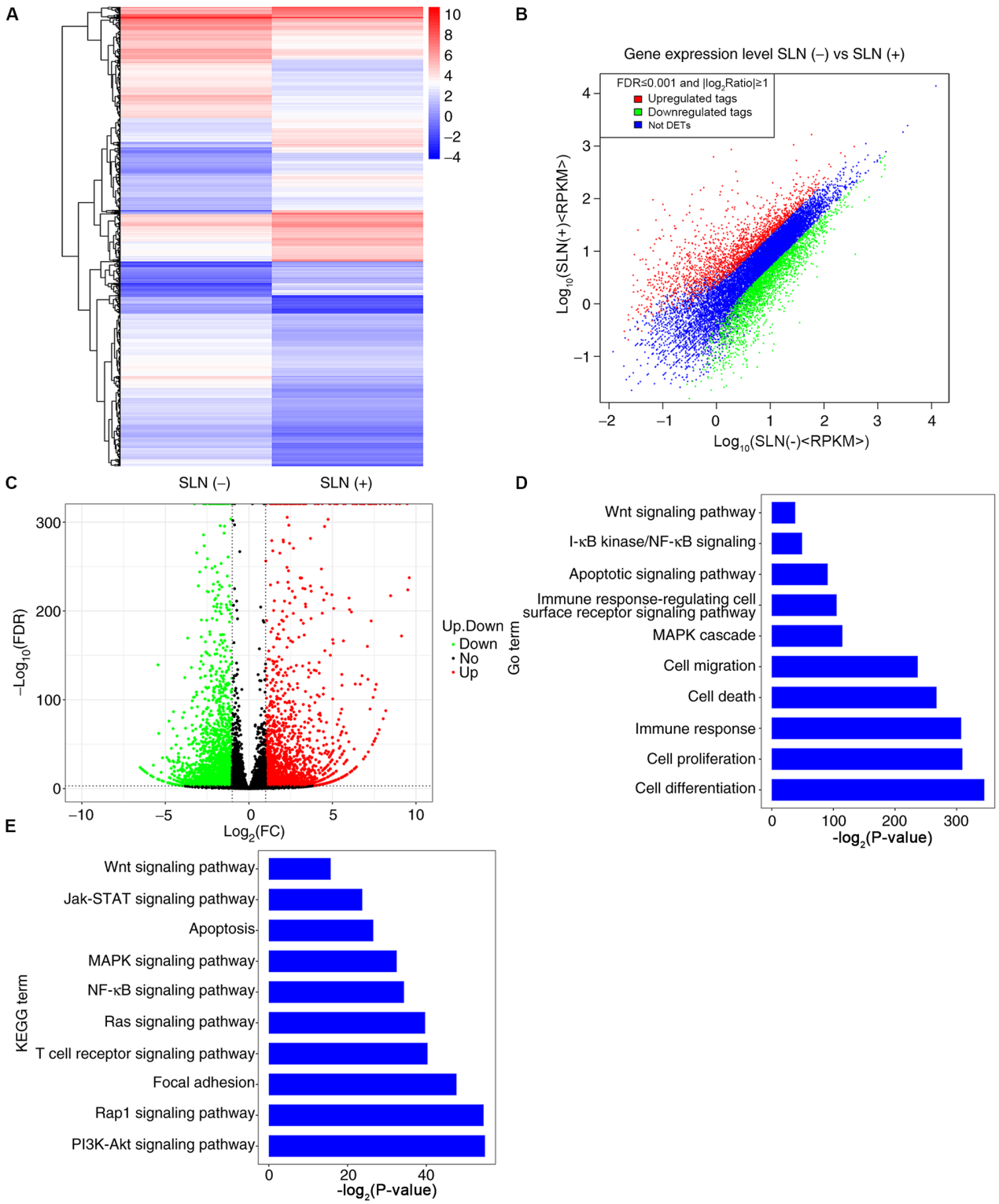

Figure 2. Differentially expressed mRNAs, and GO and KEGG analyses in patients with SLN(+) and SLN(-) metastasis. (A) Heatmap (the color indicates the value after the logarithm of the expression is taken; the red color indicates higher gene expression and the blue color indicates lower gene expression), (B) scatter plot and (C) volcano plot of the differentially expressed mRNAs in patients with SLN(+) and SLN(-) metastasis. (D) Biological processes of upregulated and downregulated mRNAs according to GO enrichment. (E) Signal pathways of upregulated and downregulated mRNAs according to KEGG pathway enrichment. GO, Gene Ontology; KEGG, Kyoto Encyclopedia of Genes and Genomes; SLN, sentinel lymph node; FDR, false discovery rate; FC, fold change; RPKM, Reads Per Kilobase of transcript per Million mapped reads; DETs, Differentially expressed tags; Jak, Janus kinase.

and lnc-GJA10-12:1 were downregulated in SLN metastasis specimens. The first identified lncRNA, lnc-ANGPTL1-3:3, is derived from the angiopoietin-like 1 (*ANGPTL1)* gene, which is a potent regulator of angiogenesis and can interact with integrin α1β1 to suppress hepatocellular carcinoma angiogenesis and metastasis via inhibition of Janus kinase 2/STAT3 signaling (33). Furthermore, the second lncRNA, lnc-GJA10-12:1, is derived from the gap junction protein

Table III. Top ten differentially expressed lncRNAs.

lncRNAs	Length, bp	SLN(-), RPKM	SLN(+), RPKM	log_2 ratio, SLN(+)/SLN(-)	Upregulation/ downregulation (SLN+/SLN-)	FDR
lnc-DDX47-3:1	2,740	0.391338128	225.814620700	9.172507504	Up	$5.90x10^{-170}$
LINC01087:1	3,516	2.744709397	779.663719700	8.150054784	Up	$0.00x10^{0}$
lnc-SLC39A11-10:48	5,836	0.183733117	50.494217380	8.102362680	Up	$3.28x10^{-79}$
TBILA:3	1,937	0.553570713	133.185239200	7.910450865	Up	$5.70x10^{-69}$
lnc-CCDC74A-8:1	1,521	3.524873343	789.454094100	7.807140148	Up	$0.00x10^{0}$
lnc-DTNBP1-16:4	73,231	0.014642248	2.978646596	7.668376078	Up	$6.65x10^{-58}$
lnc-DHCR24-1:1	503	4.263484974	748.474609300	7.455776394	Up	$4.34x10^{-100}$
lnc-CCDC74A-11:1	5,658	3.411240099	562.345523100	7.365016729	Up	$0.00x10^{0}$
lnc-ADPRHL1-5:1	509	2.106613892	309.046682100	7.196755050	Up	$4.72x10^{-41}$
lnc-IDNK-10:1	5,970	0.179609124	23.011640110	7.001359361	Up	$1.47x10^{-35}$
lnc-MB-6:1	1,733	69.298237020	0.605134684	-6.839418562	Down	$3.73x10^{-31}$
lnc-P2RX3-4:1	2,727	35.388332380	0.384561206	-6.523916736	Down	$1.18x10^{-24}$
lnc-RANBP3L-4:2	3,613	21.071386510	0.290256963	-6.181810760	Down	$4.35x10^{-19}$
lnc-TFF3-1:1	1,328	184.093942300	3.158730144	-5.864953654	Down	$4.06x10^{-61}$
lnc-TNFRSF13C-1:1	1,078	53.712791690	0.972818560	-5.786951142	Down	$3.67x10^{-14}$
lnc-NUDT12-11:1	549	99.609453600	1.910197464	-5.704488982	Down	$2.58x10^{-13}$
lnc-N4BP2-3:4	530	103.180358500	1.978676241	-5.704488982	Down	$2.58x10^{-13}$
lnc-MMP23B-1:1	1,808	27.874183710	0.580032305	-5.586652492	Down	$3.63x10^{-12}$
lnc-NDUFA10-7:1	1,024	49.215355610	1.024119539	-5.586652492	Down	$3.63x10^{-12}$
lnc-HACL1-2:1	1,778	25.932203740	0.589819127	-5.458328395	Down	$4.94x10^{-11}$

RPKM, Reads Per Kilobase of transcript per Million mapped reads; lncRNA, long non-coding RNA; FDR, false discovery rate; SLN, sentinel lymph node.

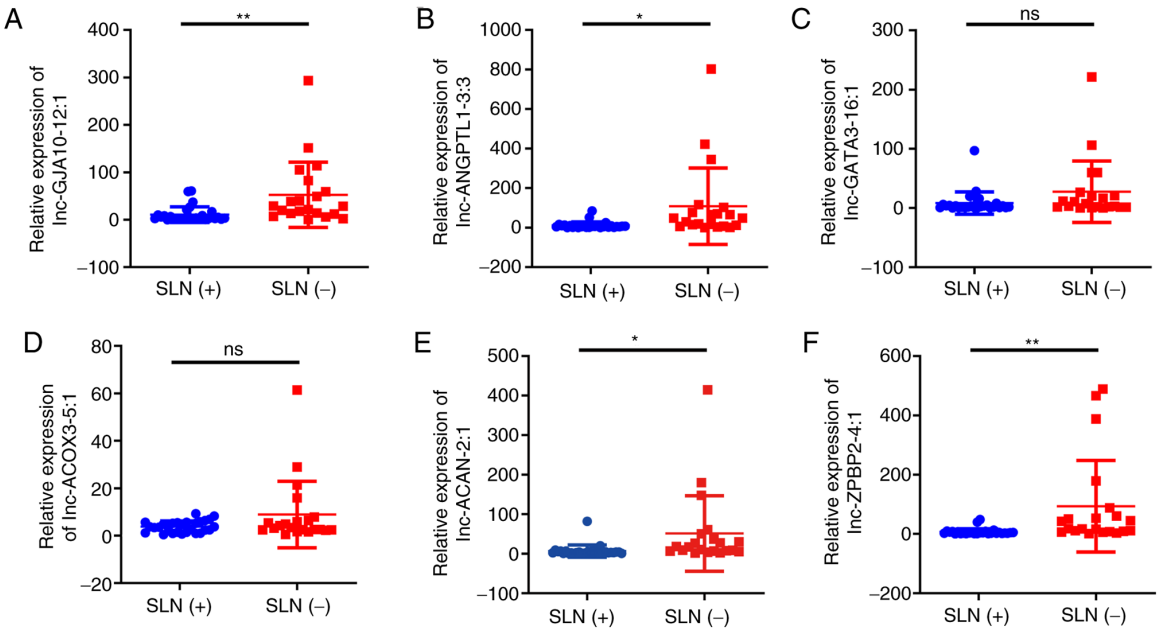

Figure 3. Quantitative PCR analysis of the six candidate lncRNAs between the SLN(+) and SLN(-) metastasis specimens. Relative expression levels of (A) lnc-GJA10-12:1, (B) lnc-ANGPTL1-3:3, (C) lnc-GATA3-16:1, (D) lnc-ACOX3-5:1, (E) lnc-ACAN-2:1 and (F) lnc-ZPBP2-4:1. *P<0.05; **P<0.01; ns, not significant. SLN, sentinel lymph node; lncRNA, long non-coding RNA.

α10 (*GJA10*) gene (34). Thus, the results of the current study indicated that both lncRNAs may potentially serve important roles in the regulation of SLN metastasis in patients with breast cancer.

Table IV. Top ten differentially expressed mRNAs.

mRNA	Gene ID	SLN(-), RPKM	SLN(+), RPKM	$\log_2$ fold-change, SLN(+)/SLN(-)	Upregulation/ downregulation (SLN+)/SLN-)	FDR
KRT19	NM_002276	0.879993293	624.542682700	9.471091928	Up	$0.00x10^{0}$
AGR2	NM_006408	1.881223855	859.243757400	8.835252123	Up	$0.00x10^{0}$
LRP2	NM_004525	0.070514511	13.785703170	7.611036966	Up	$0.00x10^{0}$
MUC16	NM_024690	0.278551308	49.981202550	7.487298711	Up	$0.00x10^{0}$
PRLR	NR_037910	0.237386784	38.441857770	7.339294629	Up	$0.00x10^{0}$
SHANK2	NR_110766	0.176387166	27.083658300	7.262533218	Up	$0.00x10^{0}$
SORD	NR_034039	2.297196335	328.383682400	7.159364465	Up	$0.00x10^{0}$
STC2	NM_003714	0.519158633	62.454697730	6.910490851	Up	$0.00x10^{0}$
EPCAM	NM_002354	1.184032220	135.573309000	6.839221026	Up	$0.00x10^{0}$
PROM1	NM_006017	0.564720687	62.228977230	6.783905243	Up	$0.00x10^{0}$
SNORD17	NR_003045	380.772408500	8.774673935	-5.439439615	Down	$4.50x10^{-140}$
LRRC55	NM_001005210	7.489998665	0.177513285	-5.398966555	Down	$7.56x10^{-63}$
SDK2	NM_001144952	4.915447389	0.179036436	-4.778997604	Down	$1.04x10^{-76}$
CNR2	NM_001841	18.023608310	0.720987293	-4.643770224	Down	$5.32x10^{-46}$
TIE1	NM_005424	5.619246835	0.241038256	-4.543042733	Down	$6.06x10^{-32}$
MARCO	NM_006770	26.302585060	1.133295762	-4.536608274	Down	$3.77x10^{-68}$
FABP4	NM_001442	74.146260690	3.245195638	-4.513996578	Down	$2.52x10^{-87}$
NPIPB3	NM_130464	5.976835270	0.265142081	-4.494544215	Down	$1.04x10^{-30}$
MAST3	NM_015016	6.150545353	0.298601665	-4.364420222	Down	$4.44x10^{-50}$
GRAP	NM_006613	21.648787300	1.101606876	-4.296604837	Down	$4.67x10^{-60}$

FDR, false discovery rate; SLN, sentinel lymph node; RPKM, reads per kilobase of transcript per million mapped reads.

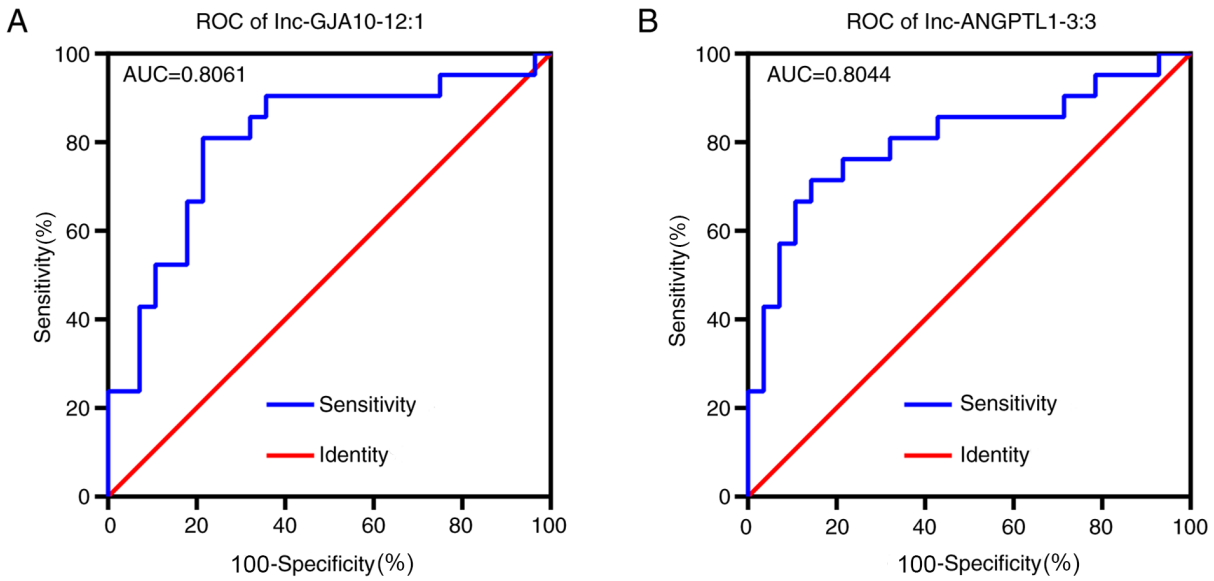

Figure 4. ROC curve analysis assessing the sensitivity and specificity of two lncRNAs, (A) lnc-GJA10-12:1 and (B) lnc-ANGPTL1-3:3. lncRNA, long non-coding RNA; ROC, receiver operating characteristic; AUC, area under the curve.

lncRNAs interact with miRNAs and can activate or suppress their functions, resulting in increased or decreased expression of their downstream targeted mRNAs (35). The GO and KEGG analyses in the present study revealed that the MAPK and PI3K/Akt signaling pathways may serve critical roles in SLN metastasis in breast cancer. Additionally, bioinformatics analysis predicted the targeted miRNAs, as well as the mRNAs. It was found that miR-302c-3p and miR-302d-3p were each targeted by both candidate lncRNAs, lnc-ANGPTL1-3:3 and lnc-GJA10-12:1, whereas miR-302a-3p and miR-302b-3p

Table V. Association of lnc-ANGPTL1-3:3 and lnc-GJA10-12:1 with patient clinicopathological features.

Groups	Cases	lnc-ANGPTL1-3:3 expression	χ^2-value	P-value	lnc-GJA10-12:1 expression	χ^2-value	P-value
Age, years						1.525	0.1345
<45	22	69.65±37.93	0.8166	0.4185	42.19±14.43		
≥45	24	40.52±15.60			19.23±5.765		
SLN metastasis						2.812	0.0074
+	26	21.32±5.312	3.574	0.0009	19.61±4.827		
-	20	188.7±93.27			71.16±31.90		
Pattern of the axillary lymph nodes						4.215	0.0001
Non-suspicious	13	149.2±67.41	2.944	0.0052	77.07±23.62		
Suspicious	33	21.16±10.50			13.92±3.269		
Tumor size, cm						0.898	0.3741
<2	6	24.51±11.61	0.5866	0.5605	12.47±5.894		
≥2	40	60.29±23.34			32.87±8.677		

lnc, long non-coding RNA; SLN, sentinel lymph node.

Table VI. Top ten miRNAs and corresponding targeted mRNAs associated with lnc-ANGPTL1-3:3.

miRNA	Specific binding sites predicted	mRNA
hsa-miR-302c-3p	306, 1284, 1993, 2215	ESR1, CCND1, BMPR2, AKT1, MICA
hsa-miR-548d-5p	960, 1053, 1491, 2264	PPARA
hsa-miR-302a-3p	306, 1281, 2215	CCND1, CCND1, CDK4, CDKN1A, LEFTY1, LEFTY2, DAZAP2, SLAIN1, TOB2, NR2F2, AKT1, TAC1, CDK2, BMI1, CDK1, MBD2, NANOG
hsa-miR-302b-3p	307, 1284, 2215	CCND2, BMI1, TGFBR2, RHOC, AKT1, HDAC4, EGFR, ERBB4, AKT2
hsa-miR-373-3p	304, 1281, 2215	RAD52, RAD23B, XPA, MRE11A, CD44, CD44, LATS2, LATS2, LATS2, LATS2, RECK, VEGFA, TXNIP, RABEP1, MYC, MBD2, RASSF1, MTOR, SIRT1, NFIB, DKK1, TGFBR2, BTG1, LEFTY1, TNFAIP1, LEFTY2
hsa-miR-520c-3p	307, 1282, 2218	APP, CD44, CD44, MTOR, SIRT1, GPC3, GPC3, MICA, EIF4G1
hsa-miR-302d-3p	306, 1284, 2218	TRPS1, KLF13, VEGFA, MBNL2, NR4A2, ERBB4, CDK2, CCND2, LEFTY1, LEFTY2, AKT1
hsa-miR-520b	308, 1283, 2219	CDKN1A, MICA, LAMTOR5, IL8, MAP3K2, CCND1, CD46, PFKP
hsa-miR-520a-3p	304, 1282, 2216	CDKN1A, PFKP
hsa-miR-520d-3p	304, 1282, 2216	EPHA2, EPHA2

miRNA/miR, microRNA.

were targeted by lnc-ANGPTL1-3:3 alone to regulate the SLN metastasis processes of breast cancer; therefore, the miR-302 family may serve an important role in SLN metastasis of lncRNA-regulated breast cancer. A previous study reported that miR-302c-3p suppressed tumorigenesis and development in hepatocellular carcinoma by targeting tumor necrosis factor receptor-associated factor 4 (36). Furthermore, AKT1 serves a crucial role as a regulator of cell invasion and proliferation in breast cancer (37-39). It has also been shown that the inhibition of AKT1 induces breast cancer metastasis via β-catenin nuclear accumulation mediated by the epidermal growth factor receptor (40). Based on the present results, it was speculated that lnc-ANGPTL1-3:3 and lnc-GJA10-12:1 may regulate two AKT1-targeting miRNAs, miR-302c-3p and miR-302d-3p, and thus control SLN metastasis in breast cancer.

MAPK, which is an important transmitter of signals from the cell surface to the nucleus, serves an important role in the development and metastasis of cancer, and it has been reported that chemokine ligand 28 promotes the growth and metastasis of breast cancer via MAPK-mediated pro-metastatic and anti-apoptotic mechanisms (41). A previous study revealed that miR-34c-3p regulated cancerous development and epithelial-mesenchymal transition of triple-negative breast cancer cells by regulating MAP3K2 signaling (42). Furthermore, in

Table VII. Top ten miRNAs and corresponding targeted mRNAs associated with lnc-GJA10-12:1.

miRNA	Specific binding sites predicted	mRNA
hsa-miR-223-3p	466, 539	RHOB, RHOB, RHOB, NFIX, E2F1, MEF2C, MEF2C, NFIA, NFIA, STMN1, STMN1, STMN1, LMO2, LMO2, Arid4b, Il6, Lpin2, CHUK, FBXW7, FBXW7, FBXW7, FBXW7, IGF1R, IGF1R, IGF1R, IGF1R, EPB41L3, SLC2A4, LIF, SP3, ARTN, FOXO1, FOXO1, HSP90B1, SCARB1, PARP1, CDK2, ECT2, PTBP2, TAL1, ATM, CYB5A, TOX, PRDM1, STAT5A, CARM1, POLR3G, FOXO3, CDC27, SP1, CCL3, IL6, CXCL2, ABCB1, CAPRIN1, PAX6, CFTR
hsa-miR-136-5p	437, 642	MTDH, BCL2
hsa-miR-34a-5p	619	SIRT1, SIRT1, SIRT1, SIRT1, SIRT1, SIRT1, SIRT1, SIRT1, SIRT1, SIRT1, VAMP2, NOTCH1, NOTCH1, NOTCH1, NOTCH1, NOTCH1, NOTCH1, NOTCH1, NOTCH1, NOTCH1, NOTCH1, NOTCH1, DLL1, DLL1, DLL1, DLL1, BCL2, BCL2, BCL2, BCL2, BCL2, BCL2, BCL2, BCL2, BCL2, BCL2, YY1, YY1, YY1, MAGEA12, MAGEA6, MAGEA3, MAGEA2, AXIN2, WNT1, WNT1, CCND1, CCND1, CCND1, CDK6, CDK6, CDK6, CDK6, CDK6, CDK6, CDK6, CDC25A, CCND3, MYCN, MYCN, MYCN, MYCN, MYCN, MYCN, E2F3, E2F3, E2F3, E2F3, E2F3, E2F3, CCNE2, CCNE2, CDK4, CDK4, CDK4, MET, MET, MET, MET, MET, MET, MET, MET, MET, MET, MYB, MYC, MYC, MYC, MYC, MAP2K1, JAG1, JAG1, JAG1, PEA15, VEGFA, IFNB1, HNF4A, HNF4A, HNF4A, Sirt1, Mycn, E2f3, NOTCH2, NOTCH2, CD44, CD44, FOXP1, FOXP1, MAP3K9, CEBPB, SPI1, ZAP70, PDGFRA, PDGFRA, PDGFRA, NANOG, SOX2, IMPA1, IMPDH2, ULBP2, SYT1, STX1A, FOSL1, FOSL1, EPHA5, AXL, AXL, CCL22, KLB, PPP1R10, BMP7, LEF1, ACSL1, GRM7, LDHA, MTA2, CDKN2A, HDAC1, HDAC1, E2F1, ACSL4, CDKN2C, SNAI1, CD24, AR, NAMPT, PDGFRB, PDGFRB, BIRC5, BIRC5, SRC, SRC, PCBP2, KDM4A, KCNH1, KLF4, MDM4, MDM4, INHBB, RICTOR, POU5F1, ARHGDIB, CYBB, HOTAIR, DGUOK, GAS1, CSF1R, KIT, SIRT7, GALNT7, IL6R, FUT8, L1CAM
hsa-miR-449b-5p	618	SIRT1, CCNE2, MET, GMNN, HDAC1, CDK4, CDC25A, CDK6
hsa-miR-449a	618	HDAC8, HDAC1, HDAC1, CDK6, CDK6, CDK6, CDC25A, CDC25A, CCND1, CCND1, HNF4A, HNF4A, GMNN, MET, MET, CCNE2, SIRT1, BCL2, BCL2, BCL2, BCL2, NOTCH1, NOTCH1, WISP2, CDK4, LEF1, E2F3, E2F3, ITPR1, MAP2K1
hsa-miR-302d-3p	420	TRPS1, KLF13, VEGFA, MBNL2, NR4A2, ERBB4, CDK2, CCND2, LEFTY1, LEFTY2, AKT1
hsa-miR-302c-3p	420	ESR1, CCND1, BMPR2, AKT1, MICA
hsa-miR-561-3p	98	NR0B1
hsa-miR-196b-5p	665	HOXB8, HOXC8, CD8A, HOXA9, HOXA9, MEIS1, FAS, ETS2, RDX, HOXB7
hsa-miR-181d-5p	679	BCL2, BCL2, HRAS, MGMT, MGMT, RAP1B

miRNA/miR, microRNA.

non-small cell lung cancer, miR-520a-3p suppresses cell proliferation, metastasis and apoptosis by targeting MAP3K2 (43), and miR-449a inhibits cell invasion by suppressing MAP2K1 (44). Based on the aforementioned studies and the present results, it was indicated that in SLN metastasis of breast cancer lnc-ANGPTL1-3:3 may target miR-520b to regulate MAP3K2 expression, and that lnc-GJA10-12:1 may target miR-34a-5p to regulate MAP2K1 and MAP3K9 expression, as well as miR-449a to regulate MAP2K1 expression.

At present, there are no mature animal models *in vivo* and cell models *in vitro* for the study of SLN metastasis. Therefore, the specific mechanism of lnc-ANGPTL1-3:3 and lnc-GJA10-12:1 regulating SLN metastasis were not investigated in the present study. In addition, the expression levels of lnc-ANGPTL1-3:3 and lnc-GJA10-12:1 in breast cancer *in situ* were not investigated in the present study. The aforementioned limitations should be investigated by future studies.

In conclusion, lnc-ANGPTL1-3:3 and lnc-GJA10-12:1 may be important regulators of SLN metastasis in breast cancer via their downregulated expression. Moreover, the present results suggested that lnc-ANGPTL1-3:3 and lnc-GJA10-12:1 may regulate the PI3K/Akt and MAPK signaling pathways by targeting the miR-302 family, miR-520a-3p, miR-34a-5p and miR-449a, which may serve a crucial role in SLN metastasis of breast cancer. It was also demonstrated that lnc-ANGPTL1-3:3

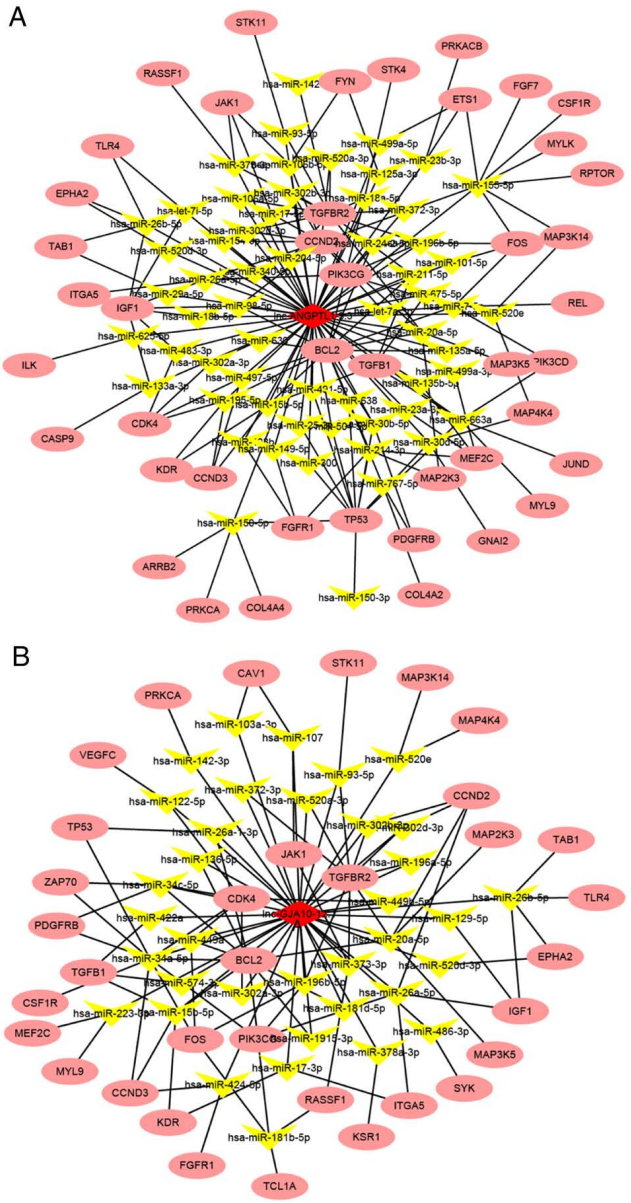

Figure 5. Regulatory networks of two lncRNAs, (A) lnc-ANGPTL1-3:3 and (B) lnc-GJA10-12:1. Regulatory networks were predicted using bioinformatics analysis. The red diamonds represent lncRNAs, the yellow diamonds represents miRNAs and the red ellipses represent mRNA. lncRNA, long non-coding RNA.

and lnc-GJA10-12:1 in SLN may serve as potential markers of breast cancer metastasis. Hence, future studies should further investigate lnc-ANGPTL1-3:3 and lnc-GJA10-12:1 expression in breast cancer tissues to provide a basis for the surgical treatment of breast cancer.

Acknowledgements

The authors would like to thank Guangzhou Forevergen Biosciences Co., Ltd. for providing technical help.

Funding

The present study was supported by the Health and Family Planning Commission of Shenzhen Municipality (grant no. SZXJ2017026), the Shenzhen 'Sanming' Project of Medicine (grant no. SZSM201512026) and Shenzhen Key Medical Discipline Construction Fund.

Availability of data and materials

The datasets used and/or analyzed during the present study are available from the corresponding author on reasonable request.

Authors' contributions

DS and JZ conceived and designed the experiments. DS, JZ, and WW performed the experiments. LL, JL, and XL analyzed the experimental data. All authors reviewed and approved the final manuscript.

Ethics approval and consent to participate

The present study was approved by the Institute Research Medical Ethics Committee of the Peking University Shenzhen Hospital (Shenzhen, China), and informed consent was provided orally and in writing by all patients.

Patient consent for publication

Not applicable.

Competing interests

The authors declare that they have no competing interests.

References

1. Bray F, Ferlay J, Soerjomataram I, Siegel RL, Torre LA and Jemal A: Global cancer statistics 2018: GLOBOCAN estimates of incidence and mortality worldwide for 36 cancers in 185 countries. CA Cancer J Clin 68: 394-424, 2018.
2. Choi HY, Park M, Seo M, Song E, Shin SY and Sohn YM: Preoperative axillary lymph node evaluation in breast cancer: Current issues and literature review. Ultrasound Q 33: 6-14, 2017.
3. Promish DI: Prediction of axillary lymph node involvement of women with invasive breast carcinoma: A multivariate analysis. Cancer 85: 1201-1203, 1999.
4. Fein DA: Identification of women with T1-T2 breast cancer at low risk of positive axillary nodes. J Surg Oncol 65: 34-39, 2015.
5. Gajdos C Tartter PI and Bleiweiss IJ: Lymphatic invasion, tumor size, and age are independent predictors of axillary lymph node metastases in women with T1 breast cancers. Ann Surg 230: 692-696, 1999.
6. Gann PH, Colilla SA, Gapstur SM, Winchester DJ and Winchester DP: Factors associated with axillary lymph node metastasis from breast carcinoma: Descriptive and predictive analyses. Cancer 86: 1511-1519, 2015.
7. Rivadeneira DE, Simmons RM, Christos PJ, Hanna K, Daly JM and Osborne MP: Predictive factors associated with axillary lymph node metastases in T1a and T1b breast carcinomas: Analysis in more than 900 patients. J Am Coll Surg 191: 1-6; Discussion 6-8, 2000.
8. Tabár L, Chen HH, Duffy SW, Yen MF, Chiang CF, Dean PB and Smith RA: A novel method for prediction of long-term outcome of women with T1a, T1b, and 10-14 mm invasive breast cancers: A prospective study. Lancet 355: 429-433, 2000.
9. Wong JH: Sentinel lymphadenectomy in breast cancer: University research tool or community practice? Surg Clin North Am 80: 1821-1830, 2000.
10. Cserni G, Boross G and Baltás B: The role of the histopathological analysis of sentinel lymph nodes in breast cancer. Preliminary findings. Orv Hetil 139: 1899-1903, 1998 (In Hungarian).

11. Lucci A, McCall LM, Beitsch PD, Whitworth PW, Reintgen DS, Blumencranz PW, Leitch AM, Saha S, Hunt KK and Giuliano AE; American College of Surgeons Oncology Group: Surgical complications associated with sentinel lymph node dissection (SLND) plus axillary lymph node dissection compared with SLND alone in the American College of Surgeons Oncology Group Trial Z0011. J Clin Oncol 25: 3657-3663, 2007.
12. Veronesi U: A randomized comparison of sentinel-node biopsy with routine axillary dissection in breast cancer. N Engl J Med 349: 546-553, 2005.
13. Giuliano AE, Haigh PI, Brennan MB, Hansen NM, Kelley MC, Ye W, Glass EC and Turner RR: Prospective observational study of sentinel lymphadenectomy without further axillary dissection in patients with sentinel node-negative breast cancer. J Clin Oncol 18: 2553-2559, 2000.
14. Burak WE, Hollenbeck ST, Zervos EE, Hock KL, Kemp LC and Young DC: Sentinel lymph node biopsy results in less postoperative morbidity compared with axillary lymph node dissection for breast cancer. Am J Surg 183: 23-27, 2002.
15. Haid A, Kuehn T, Konstantiniuk P, Köberle-Wührer R, Knauer M, Kreienberg R and Zimmermann G: Shoulder-arm morbidity following axillary dissection and sentinel node only biopsy for breast cancer. Eur J Surg Oncol 28: 705-710, 2002.
16. Schrenk P, Rieger R, Shamiyeh A and Wayand W: Morbidity following sentinel lymph node biopsy versus axillary lymph node dissection for patients with breast carcinoma. Cancer 88: 608-614, 2000.
17. Temple LK, Baron R, Cody HS III, Fey JV, Thaler HT, Borgen PI, Heerdt AS, Montgomery LL, Petrek JA and Van Zee KJ: Sensory morbidity after sentinel lymph node biopsy and axillary dissection: A prospective study of 233 women. Ann Surg Oncol 9: 654-662, 2002.
18. Yang L, Lin C, Jin C, Yang JC, Tanasa B, Li W, Merkurjev D, Ohgi KA, Meng D, Zhang J, *et al*: lncRNA-dependent mechanisms of androgen-receptor-regulated gene activation programs. Nature 500: 598-602, 2013.
19. Huarte M: The emerging role of lncRNAs in cancer. Nat Med 21: 1253-1261, 2015.
20. Yan X, Zhang D, Wu W, Wu S, Qian J, Hao Y, Yan F, Zhu P, Wu J, Huang G, *et al*: Mesenchymal stem cells promote hepatocarcinogenesis via lncRNA-MUF interaction with ANXA2 and miR-34a. Cancer Res 77: 6704-6716, 2017.
21. Yin J, Luo W, Zeng X, Zeng L, Li Z, Deng X, Tan X and Hu W: UXT-AS1-induced alternative splicing of UXT is associated with tumor progression in colorectal cancer. Am J Cancer Res 7: 462-472, 2017.
22. Martens-Uzunova ES, Böttcher R, Croce CM, Jenster G, Visakorpi T and Calin GA: Long noncoding RNA in prostate, bladder, and kidney cancer. Eur Urol 65: 1140-1151, 2014.
23. Ellinger J, Alam J, Rothenburg J, Deng M, Schmidt D, Syring I, Miersch H, Perner S and Müller SC: The long non-coding RNA lnc-ZNF180-2 is a prognostic biomarker in patients with clear cell renal cell carcinoma. Am J Cancer Res 5: 2799, 2015.
24. Shi J, Li X, Zhang F, Zhang C, Guan Q, Cao X, Zhu W, Zhang X, Cheng Y, Ou K, *et al*: Circulating lncRNAs associated with occurrence of colorectal cancer progression. Am J Cancer Res 5: 2258-2265, 2015.
25. Zhang K, Shi H, Xi H, Wu X, Cui J, Gao Y, Liang W, Hu C, Liu Y, Li J, *et al*: Genome-wide lncRNA microarray profiling identifies novel circulating lncRNAs for detection of gastric cancer. Theranostics 7: 213-227, 2017.
26. Shen X, Bai Y, Luo B and Zhou X: Upregulation of lncRNA BANCR associated with the lymph node metastasis and poor prognosis in colorectal cancer. Biol Res 50: 32, 2017.
27. Kong Q and Qiu M: Long noncoding RNA SNHG15 promotes human breast cancer proliferation, migration and invasion by sponging miR-211-3p. Biochem Biophys Res Commun 495: 1594-1600, 2018.
28. Pan Y, Pan Y, Cheng Y, Yang F, Yao Z and Wang O: Knockdown of LncRNA MAPT-AS1 inhibites proliferation and migration and sensitizes cancer cells to paclitaxel by regulating MAPT expression in ER-negative breast cancers. Cell Biosci 8: 7, 2018.
29. Gershenwald JE, Scolyer RA, Hess KR, Sondak VK, Long GV, Ross MI, Lazar AJ, Faries MB, Kirkwood JM, McArthur GA, *et al*: Melanoma staging: Evidence-based changes in the American Joint Committee on Cancer eighth edition cancer staging manual. CA Cancer J Clin 67: 472-492, 2017.
30. Wang X, Liu J, Zhou G, Guo J, Yan H, Niu Y, Li Y, Yuan C, Geng R, Lan X, *et al*: Whole-genome sequencing of eight goat populations for the detection of selection signatures underlying production and adaptive traits. Sci Rep 6: 38932, 2016.
31. Livak KJ and Schmittgen TD: Analysis of relative gene expression data using real-time quantitative PCR and the 2(-Delta Delta C(T)) method. Methods 25: 402-408, 2001.
32. Sui J, Li YH, Zhang YQ, Li CY, Shen X, Yao WZ, Peng H, Hong WW, Yin LH, Pu YP and Liang GY: Integrated analysis of long non-coding RNA-associated ceRNA network reveals potential lncRNA biomarkers in human lung adenocarcinoma. Int J Oncol 49: 2023-2036, 2016.
33. Yan Q, Jiang L, Liu M, Yu D, Zhang Y, Li Y, Fang S, Li Y, Zhu YH, Yuan YF and Guan XY: ANGPTL1 interacts with integrin α1β1 to suppress HCC angiogenesis and metastasis by inhibiting JAK2/STAT3 signaling. Cancer Res 77: 5831-5845, 2017.
34. Söhl G, Nielsen PA, Eiberger J and Willecke K: Expression profiles of the novel human connexin genes hCx30.2, hCx40.1, and hCx62 differ from their putative mouse orthologues. Cell Commun Adhes 10: 27-36, 2003.
35. Xiao B, Zhang W, Chen L, Hang J, Wang L, Zhang R, Liao Y, Chen J, Ma Q, Sun Z and Li L: Analysis of the miRNA-mRNA-lncRNA network in human estrogen receptor-positive and estrogen receptor-negative breast cancer based on TCGA data. Gene 658: 28-35, 2018.
36. Yang L, Guo Y, Liu X, Wang T, Tong X, Lei K, Wang J, Huang D and Xu Q: The tumor suppressive miR-302c-3p inhibits migration and invasion of hepatocellular carcinoma cells by targeting TRAF4. J Cancer 9: 2693-2701, 2018.
37. Cejalvo JM, Pérez-Fidalgo JA, Ribas G, Burgués O, Mongort C, Alonso E, Ibarrola-Villava M, Bermejo B, Martínez MT, Cervantes A and Lluch A: Clinical implications of routine genomic mutation sequencing in PIK3CA/AKT1 and KRAS/NRAS/BRAF in metastatic breast cancer. Breast Cancer Res Treat 160: 69-77, 2016.
38. Chin YR and Toker A:The actin-bundling protein palladin is an Akt1-specific substrate that regulates breast cancer cell migration. Mol Cell 38: 333-344, 2010.
39. Liu H, Radisky DC, Nelson CM, Zhang H, Fata JE, Roth RA and Bissell MJ: Mechanism of Akt1 inhibition of breast cancer cell invasion reveals a protumorigenic role for TSC2. Proc Natl Acad Sci USA 103: 4134-4139, 2006.
40. Li W, Hou JZ, Niu J, Xi ZQ, Ma C, Sun H, Wang CJ, Fang D, Li Q and Xie SQ: Akt1 inhibition promotes breast cancer metastasis through EGFR-mediated beta-catenin nuclear accumulation. Cell Commun Signal 16: 82, 2018.
41. Yang XL, Liu KY, Lin FJ, Shi HM and Ou ZL: CCL28 promotes breast cancer growth and metastasis through MAPK-mediated cellular anti-apoptosis and pro-metastasis. Oncol Rep 38: 1393-1401, 2017.
42. Wu J, Li WZ, Huang ML, Wei HL, Wang T, Fan J, Li NL and Ling R: Regulation of cancerous progression and epithelial-mesenchymal transition by miR-34c-3p via modulation of MAP3K2 signaling in triple-negative breast cancer cells. Biochem Biophys Res Commun 483: 10-16, 2017.
43. Yu J, Tan Q, Deng B, Fang C, Qi D and Wang R: The microRNA-520a-3p inhibits proliferation, apoptosis and metastasis by targeting MAP3K2 in non-small cell lung cancer. Am J Cancer Res 5: 802-811, 2015.
44. You J, Zhang Y, Li Y, Fang N, Liu B, Zu L and Zhou Q: MiR-449a suppresses cell invasion by inhibiting MAP2K1 in non-small cell lung cancer. Am J Cancer Res 5: 2730-2744, 2015.